SAND2022-5002C

Exceptional service in the national interest

Sandia National Laboratories

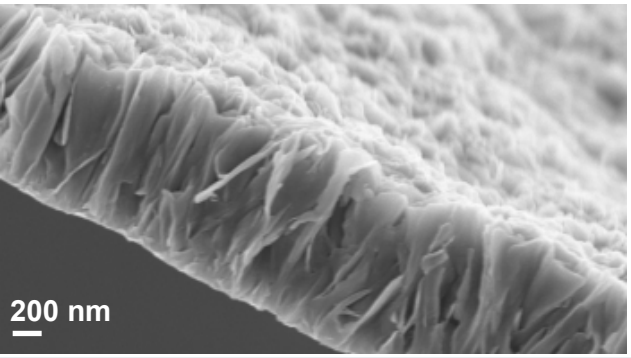

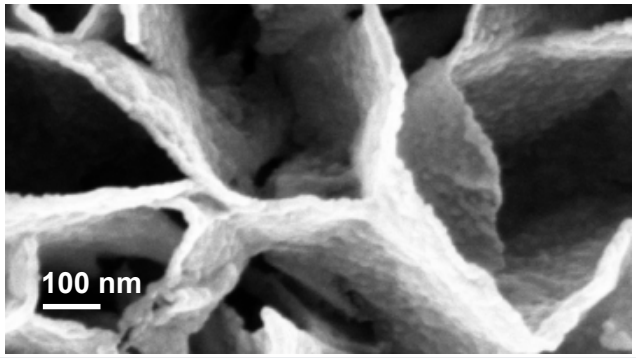

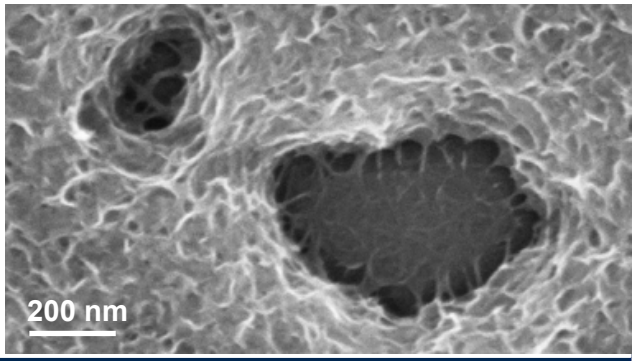

Advances in manganese- and cobalt-based nanostructures for oxygen/hydrogen electrocatalysis

Julian A. Vigil and Timothy N. Lambert

Materials, Devices & Energy Technologies
Sandia National Laboratories

American Chemical Society National Meeting
San Francisco, CA; April 3, 2017 (3:45 PM)

U.S. DEPARTMENT OF ENERGY

NNSA National Nuclear Security Administration

Sandia National Laboratories is a multi-program laboratory managed and operated by Sandia Corporation, a wholly owned subsidiary of Lockheed Martin Corporation, for the U.S. Department of Energy's National Nuclear Security Administration under contract DE-AC04-94AL85000. SAND NO. 2011-XXXXP

Next-gen energy conversion & storage

Sandia National Laboratories

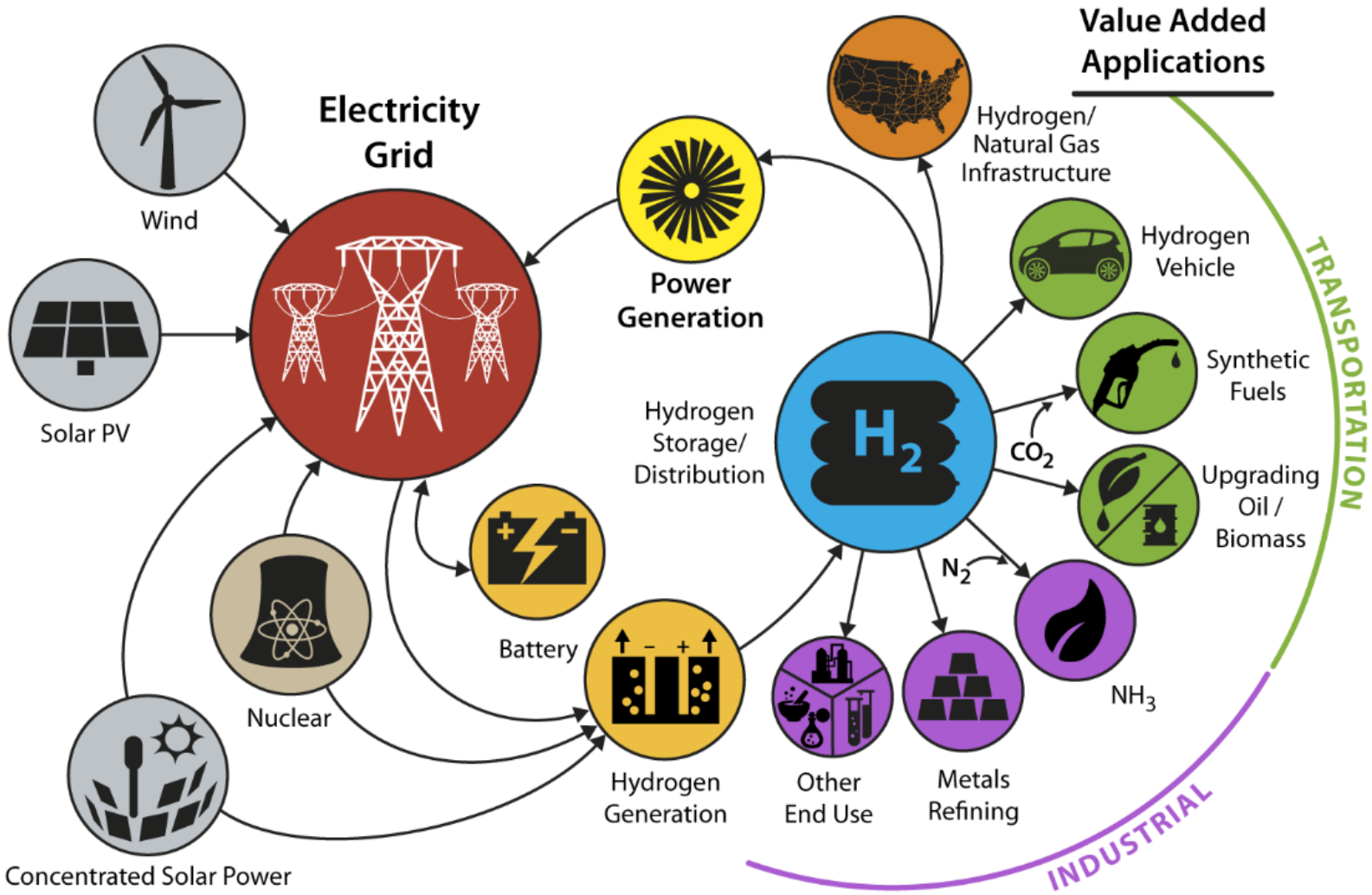

Adapted from: "H_2 at Scale: Deeply Decarbonizing our Energy System," DOE H_2 at Scale HTAC 040616. https://www.hydrogen.energy.gov/pdfs/htac_apr16_10_pivovar.pdf.

Next-gen energy conversion & storage

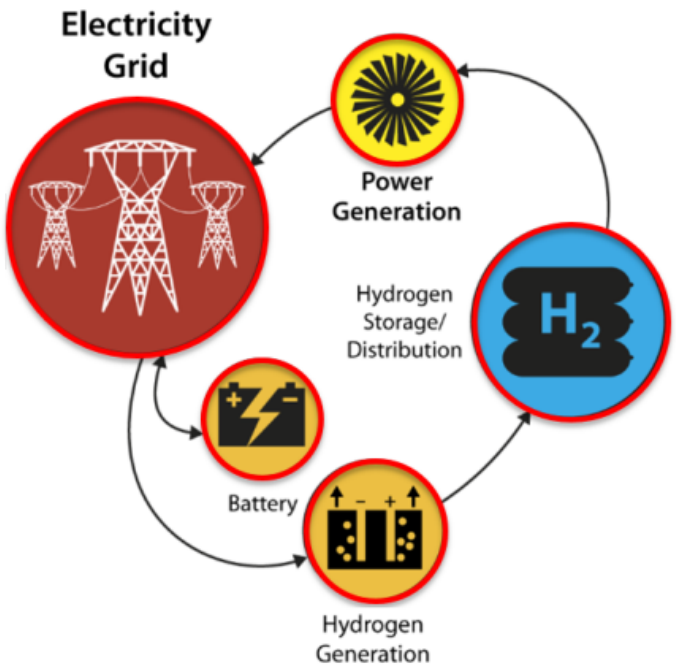

Energy conversion (and storage) steps limited by kinetics of electrochemical reactions

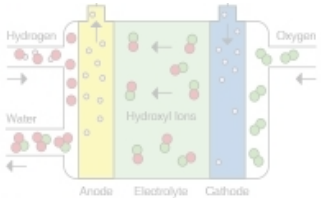

Alkaline fuel cell

Anode: $2H_2 + 4OH^- \rightarrow 4H_2O + 4e^-$

Cathode: $O_2 + 2H_2O + 4e^- \rightarrow 4OH^-$

Overall: $2H_2 + O_2 \rightarrow 2H_2O$

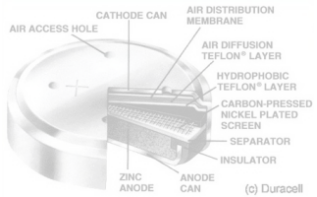

Secondary Zn-air battery

Anode: $2Zn \leftrightarrow 2Zn^{2+} + 4e^-$

Cathode: $O_2 + 2H_2O + 4e^- \leftrightarrow 4OH^-$

Overall: $2Zn + O_2 + 2H_2O \leftrightarrow 2Zn^{2+} + 4OH^-$

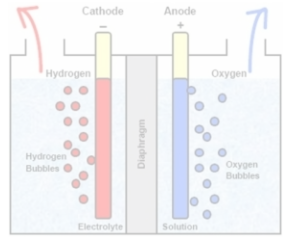

Alkaline electrolyzer

Anode: $4OH^- \rightarrow O_2 + 2H_2O + 4e^-$

Cathode: $4H_2O + 4e^- \rightarrow 2H_2 + 4OH^-$

Overall: $2H_2O \rightarrow 2H_2 + O_2$

Next-gen energy conversion & storage

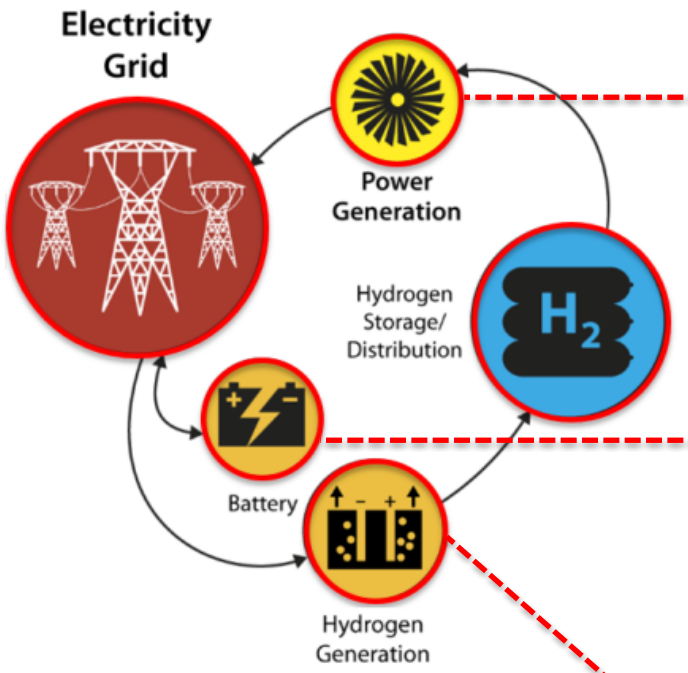

Energy conversion (and storage) steps <u>limited by kinetics of electrochemical reactions</u>

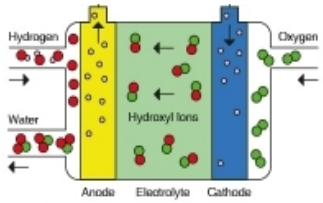

Alkaline fuel cell

Anode: $2H_2 + 4OH^- \rightarrow 4H_2O + 4e^-$ (1)

Cathode: $O_2 + 2H_2O + 4e^- \rightarrow 4OH^-$ (2)

Overall: $2H_2 + O_2 \rightarrow 2H_2O$

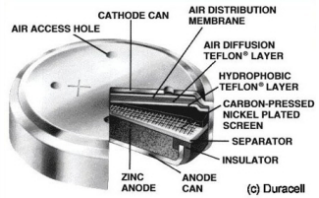

Secondary Zn-air battery

Anode: $2Zn \leftrightarrow 2Zn^{2+} + 4e^-$

Cathode: $O_2 + 2H_2O + 4e^- \leftrightarrow 4OH^-$ (2)

Overall: $2Zn + O_2 + 2H_2O \leftrightarrow 2Zn^{2+} + 4OH^-$

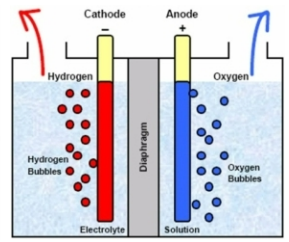

Alkaline electrolyzer

Anode: $4OH^- \rightarrow O_2 + 2H_2O + 4e^-$ (2)

Cathode: $4H_2O + 4e^- \rightarrow 2H_2 + 4OH^-$ (1)

Overall: $2H_2O \rightarrow 2H_2 + O_2$

(1) **Hydrogen oxidation/ evolution (HOR/ HER)** (2) **Oxygen reduction/ evolution (ORR/ OER)**

Adapted from: "H_2 at Scale: Deeply Decarbonizing our Energy System," DOE H_2 at Scale HTAC 040616. https://www.hydrogen.energy.gov/pdfs/htac_apr16_10_pivovar.pdf.

Manganese oxide for the ORR

Sandia National Laboratories

Oxygen reduction (ORR)

$$O_2 + 2H_2O + 4e^- \underset{\text{OER}}{\overset{\text{ORR}}{\rightleftharpoons}} 4OH^- \qquad E^o = +1.23\ \text{V vs. RHE}$$

Commercial catalyst materials: ***Pt, Pt/C ($$)***

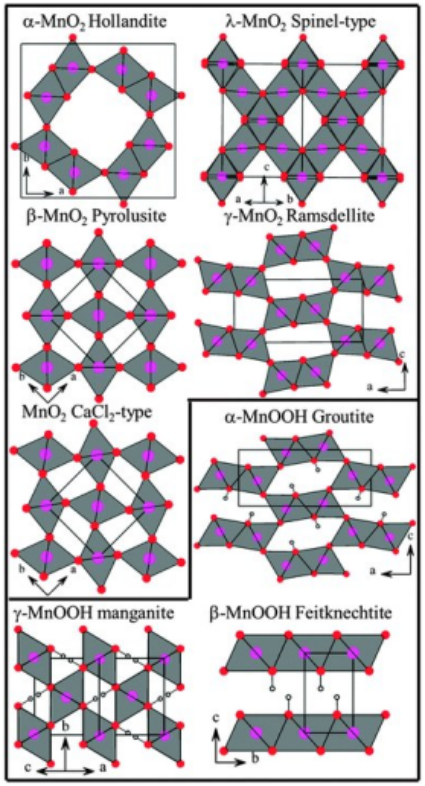

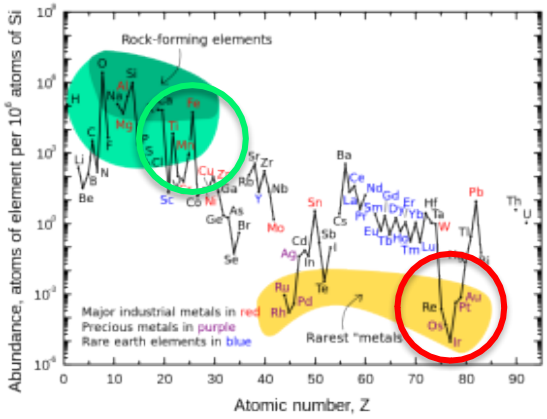

Mn abundance

Range of stable MnO_x crystal structures: valence, octahedral configuration, etc.

Intrinsic

Surface valence:

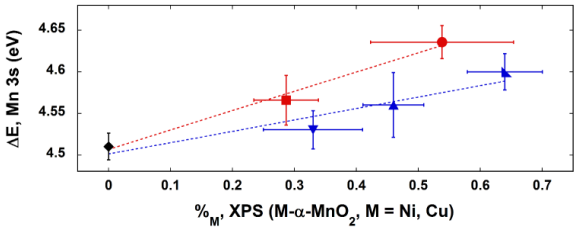

Lambert *et al. J. Phys. Chem. C*, **2017**, 121 (5), pp 2789–2797

Oxygen vacancy:

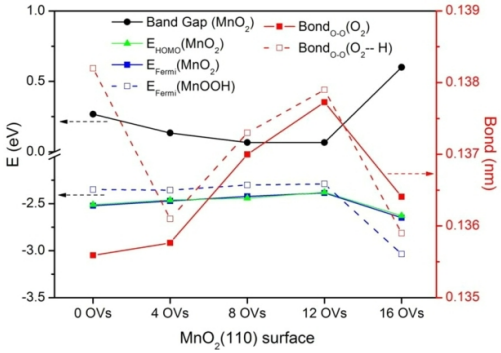

Li *et al. ACS Catal.*, **2015**, 5 (8), pp 4825–4832

Extrinsic

Carbon blending/ growth:

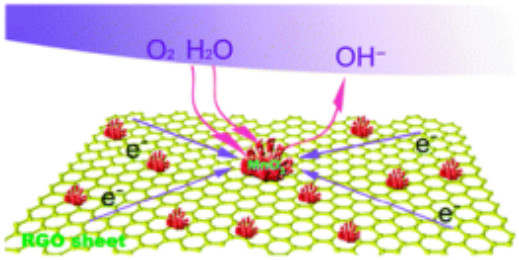

Zhang *et al. Chem. Commun.*, 2013, **49**, 6334-6336

Manganese oxide for the ORR

Sandia National Laboratories

Oxygen reduction (ORR)

$$O_2 + 2H_2O + 4e^- \underset{\text{OER}}{\overset{\text{ORR}}{\rightleftharpoons}} 4OH^- \qquad E^o = +1.23\ \text{V vs. RHE}$$

Commercial catalyst materials: ***Pt, Pt/C ($$)***

(i) Direct four electron pathway:
$O_2 + 2H_2O + 4e^- \rightarrow 4OH^-$

(ii) Indirect (peroxide) pathway:
$O_2 + H_2O + 2e^- \rightarrow OH^- + HO_2^-$

followed by either

(ii-a) the further reduction of peroxide:
$HO_2^- + H_2O + 2e^- \rightarrow 3\ OH^-$

(ii-b) the catalytic peroxide decomposition:
$HO_2^- \rightarrow ½\ O_2 + OH^-$

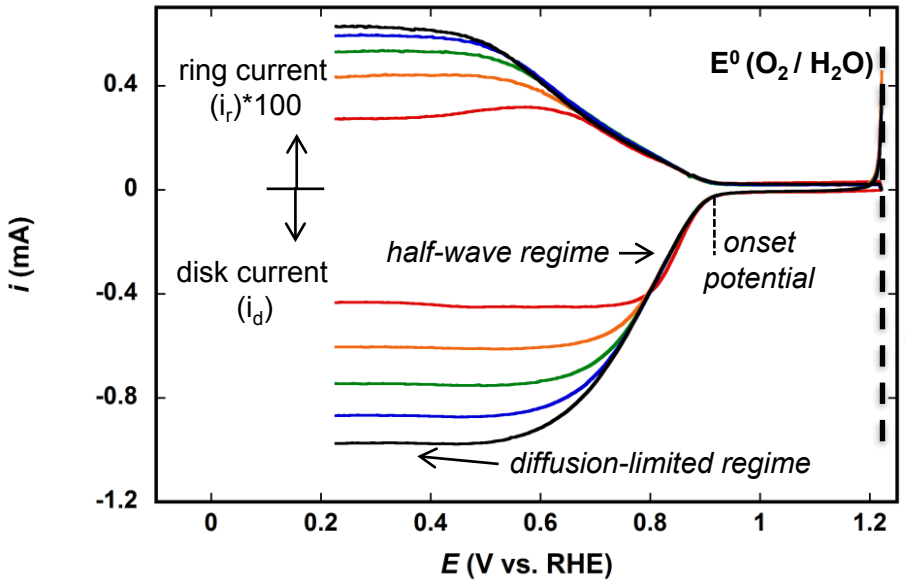

Koutecky-Levich theory for RDE

$$\frac{1}{i} = \frac{1}{i_k} + \frac{1}{i_d}$$

$$= -\frac{1}{nFAkC^0} - \frac{1}{0.62nFAD_{O_2}^{2/3}\upsilon^{-1/6}C^0\omega^{1/2}}$$

Quantifying HO_2^- (and n) with RRDE

$$\%(HO_2^-) = \frac{200\left(\frac{i_r}{N}\right)}{\left(\frac{i_r}{N} + i_d\right)} \qquad n = \frac{4(i_d)}{\left(\frac{i_r}{N} + i_d\right)}$$

Yu et al., ACS Appl. Mater. Interfaces, 2016, 8, 35264-35269

Manganese oxide for the ORR

Sandia National Laboratories

Particle size/morphology effects:

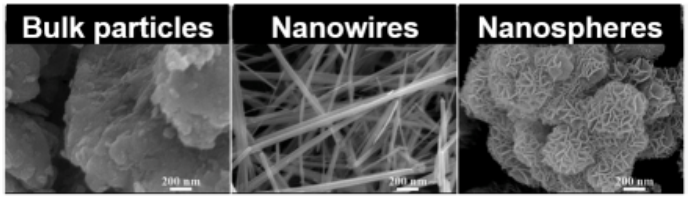

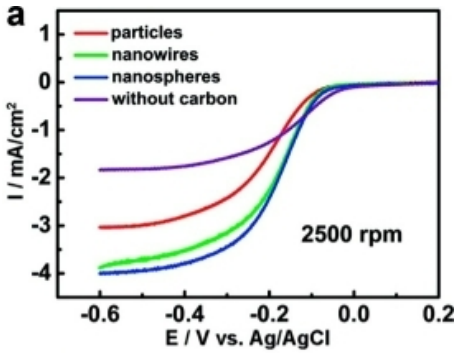

- ORR activity increases with BET surface area
- Decrease in current without carbon

F. Cheng *et al. Chem. Mater.* **2010**, *22*, 898–905

Phase-dependent activity:

- ORR activity increases with average Mn valence
- α most active phase of MnO_2

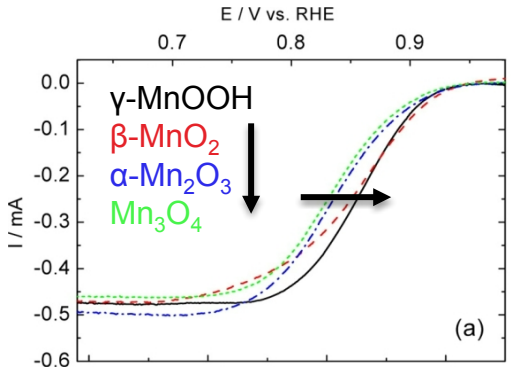

MnO_2 ~ MnOOH > Mn_2O_3 > Mn_3O_4

Tang *et al. ACS Catal.* **2014**, *4 (2)*, pp 457 - 463

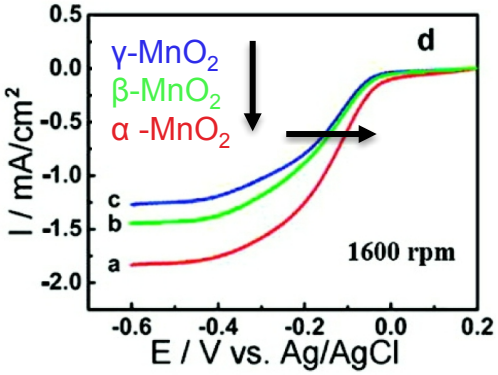

α-MnO_2 > β-MnO_2 > γ-MnO_2

F. Cheng *et al. Chem. Mater.* **2010**, *22*, 898–905

Further modification:
substitutional doping to tune valence?
interparticle contact resistance in nanostructures?

α-MnO_2 nanowires and cation doping

Sandia National Laboratories

$$MnSO_{4\,(aq)} + KMnO_{4\,(aq)} \xrightarrow{140\,^{\circ}C,\ 120\,h} \alpha - MnO_{2\,(s)}\ (NWs)$$

$$\mathbf{MnSO_{4\,(aq)} + KMnO_{4\,(aq)} + \begin{matrix} Ni \\ Cu \end{matrix}(NO_3)_{2\,(aq)} \xrightarrow{140\,^{\circ}C,\ 120\,h} \begin{matrix} Ni \\ Cu \end{matrix} - \alpha - MnO_{2\,(s)}\ (NWs)}$$

α-MnO_2 Ni-α-MnO_2 Cu-α-MnO_2

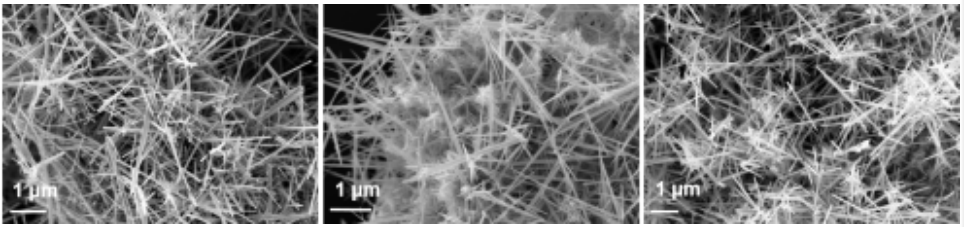

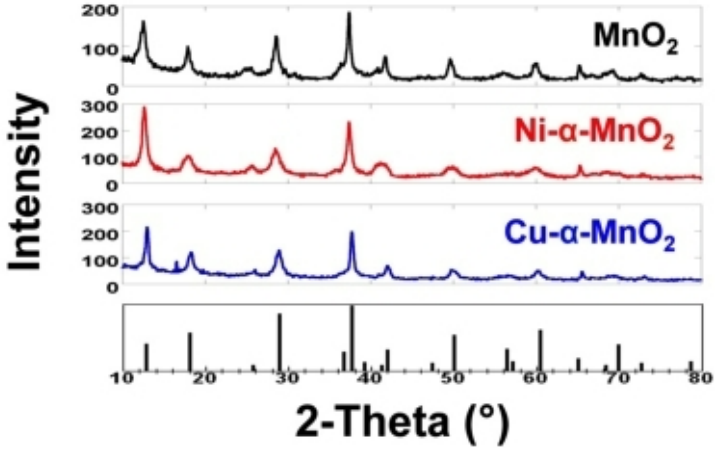

→ **phase and morphology retention**

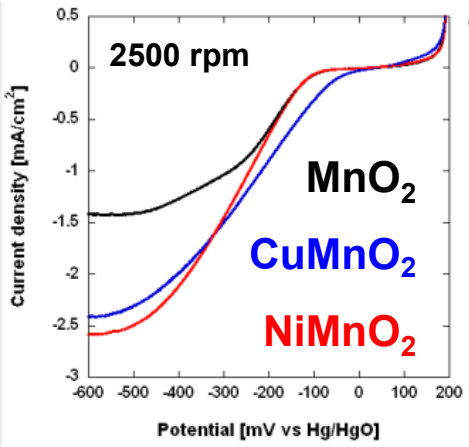

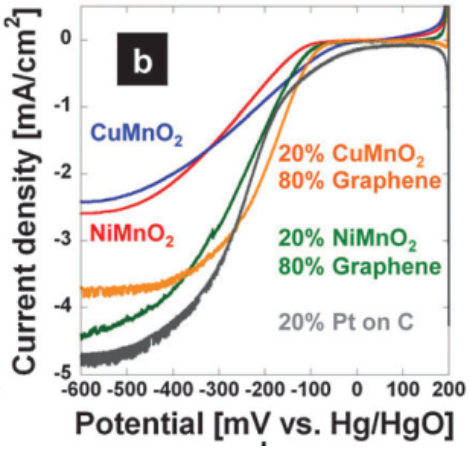

Origin of increased activity?
→ crystal structure
→ electronic structure
→ conductivity

Effects of Cu-doping on crystal structure

Tunable Cu doping demonstrated by changing precursor ratios (Cu^{2+} : Mn^{2+})
→ **0 – 3 % bulk Cu, 0 – 0.7 % surface Cu**

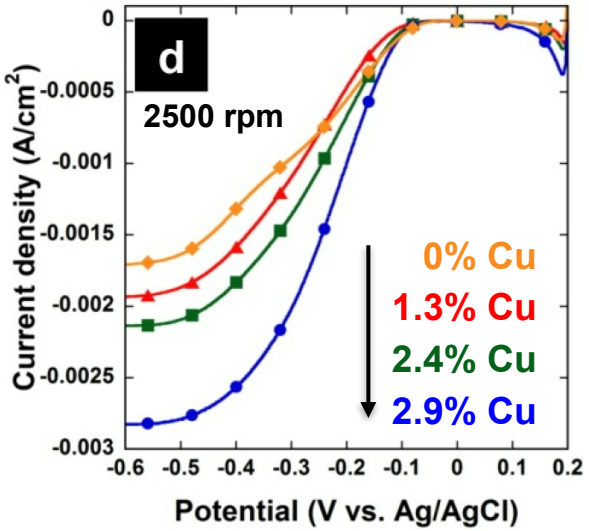

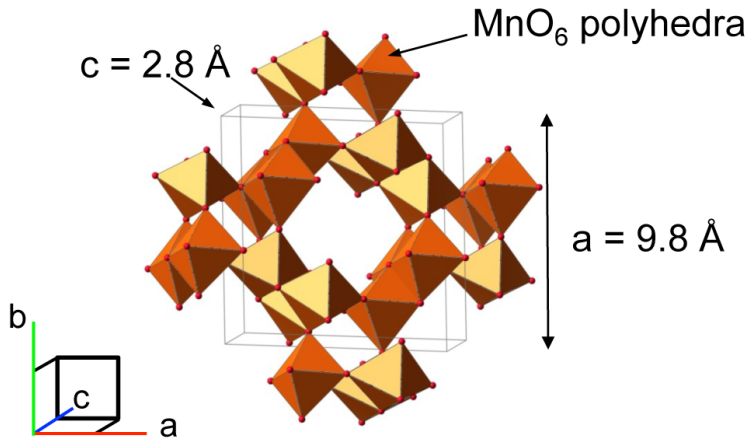

Hollandite (α-MnO_2)
Cryptomellane (α-MnO_2 w/ K^+ in channels)
Tetragonal
2 x 2 channels

- **Bond Lengths** (*higher covalency)*
  Cu 2.9-α-MnO_2 (1.900 ± 0.010 Å)
  α-MnO_2 (1.915 ± 0.035 Å)

- **Lattice volume** (*lattice expansion)*
  Cu 2.9-α-MnO_2 (278.12 $Å^3$)
  α-MnO_2 (276.45 $Å^3$)

- **Crystallite size** (more edge defects)
  Cu 2.9-α-MnO_2 (16 nm)
  α-MnO_2 (36 nm)

Electronic effect: Importance of Mn^{3+}

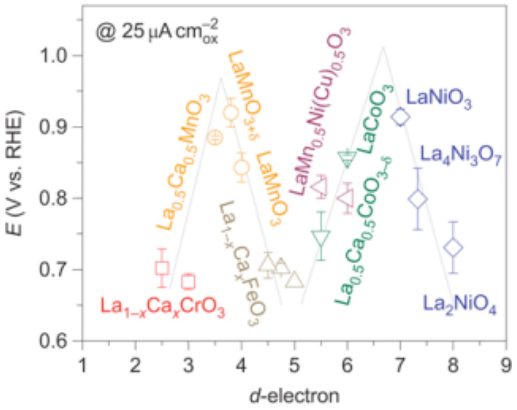

J. Suntivich *et al. Nature Chemistry* **2011** *3*, 546-550.

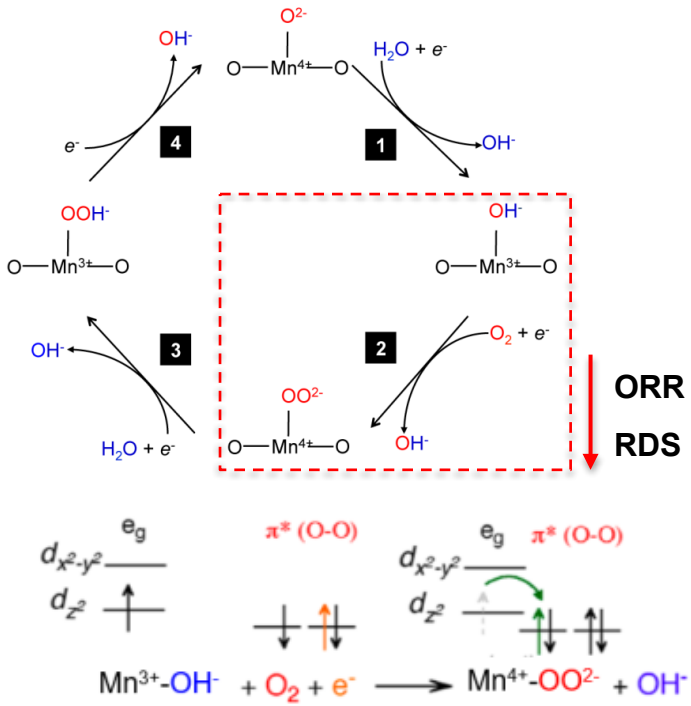

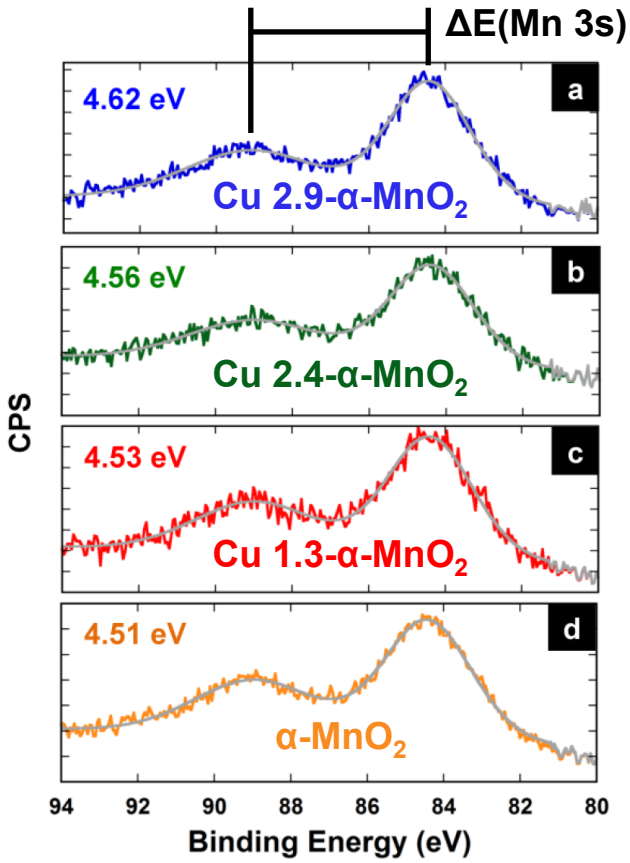

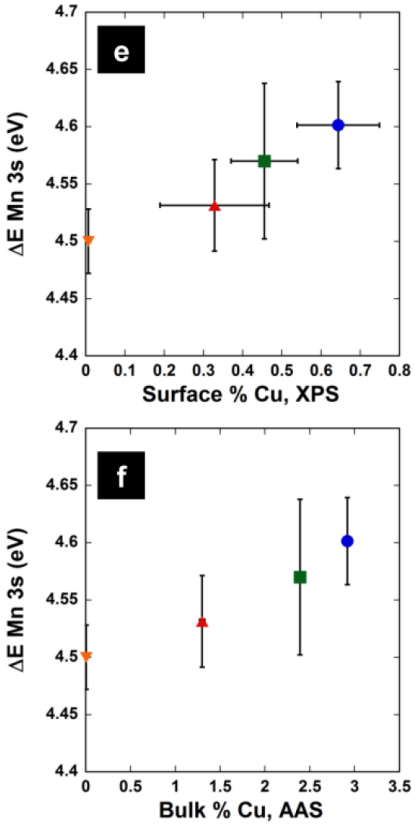

- Mn 3s multiplet splitting readily correlates with Mn valence: ΔE(Mn 3s)
- ΔE(Mn 3s) trends with % Cu – Cu increases surface Mn^{3+}

Electronic effect: Importance of Mn^{3+}

Tunable Ni doping also demonstrated from precursor ratios (Ni^{2+} : Mn^{2+})
→ **0 – 5 % bulk Ni, 0 – 0.6 % surface Ni**

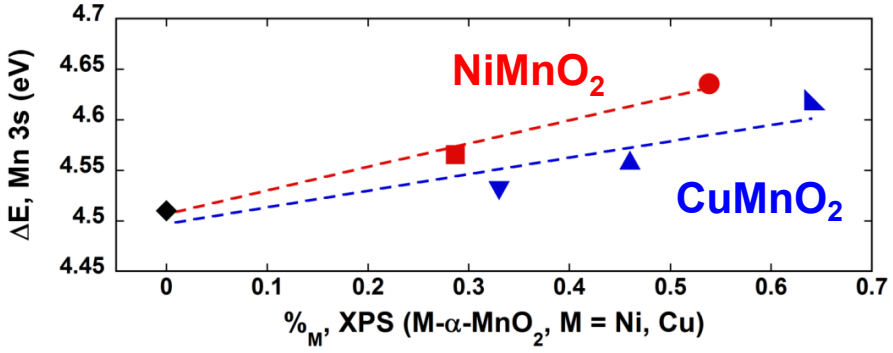

- Ni^{2+} dopant more effective at increasing surface Mn^{3+} concentration than Cu^{2+} dopant
  - Ni^{2+}: 0.69 Å
  - Cu^{2+}: 0.73 Å
  - Mn^{3+}: 0.65 Å Mn^{4+}: 0.53 Å

→ electrocatalytic activity trends with ΔE(Mn 3s) and independent of the cation

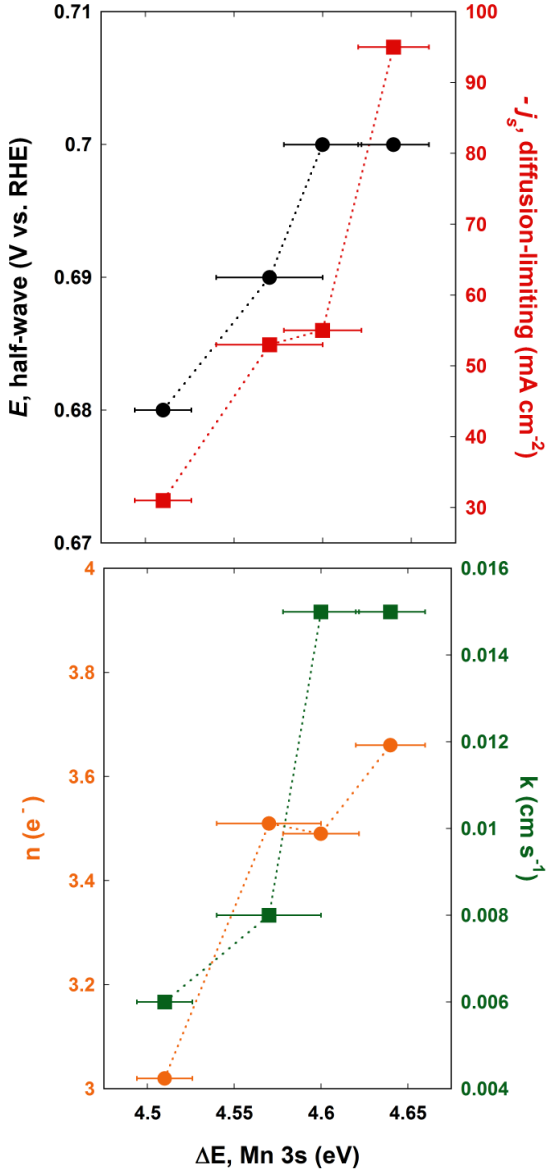

Single Nanowire Conductivity

Sandia National Laboratories

Methodology:

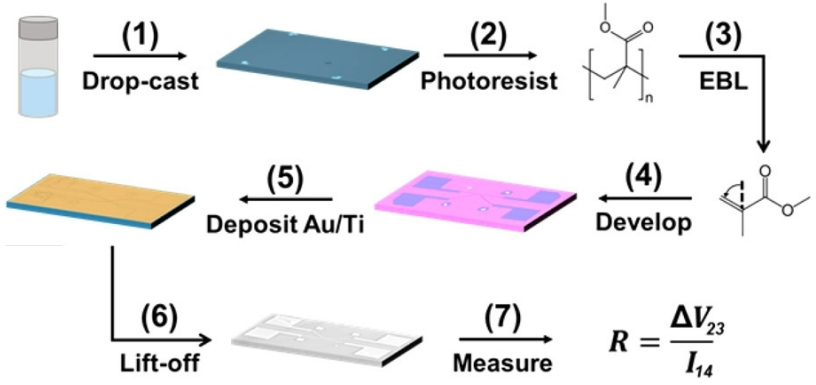

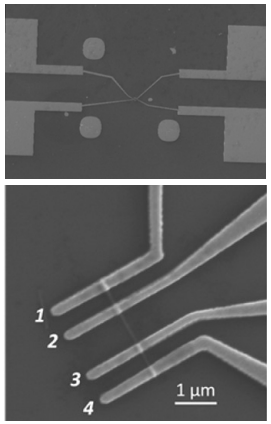

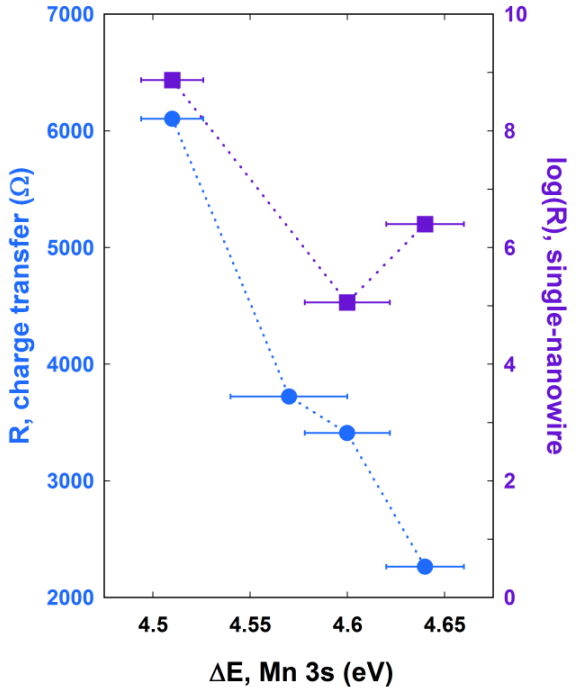

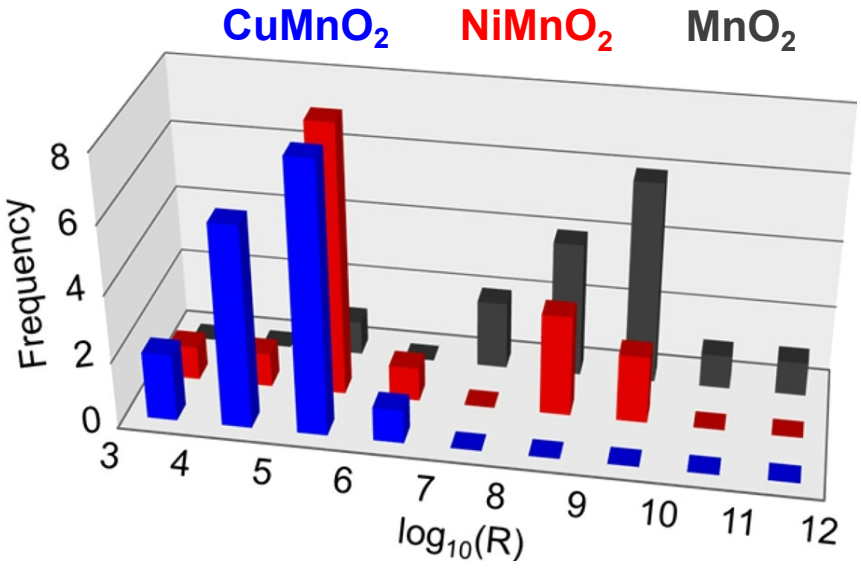

- Cu-doped MnO_2 nanowires less resistive
- EIS-derived charge transfer resistance may be more appropriate

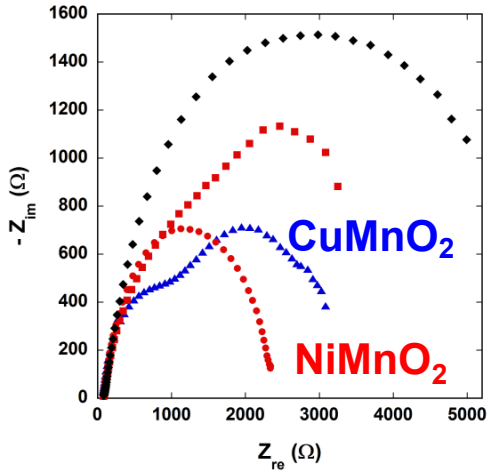

Conductive polymer hybrids: PEDOT

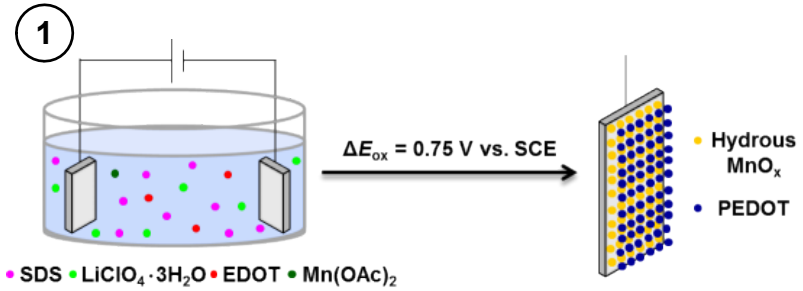

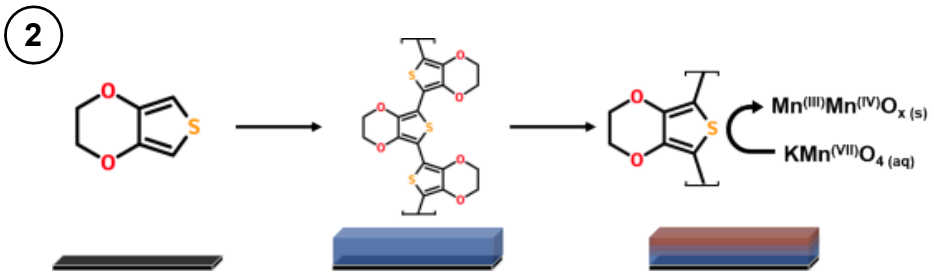

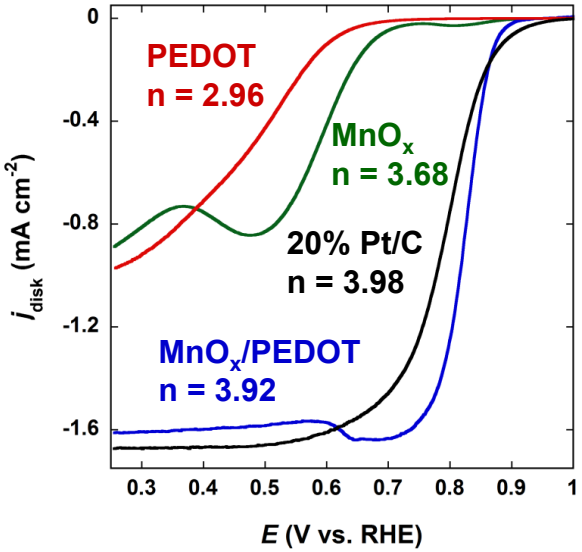

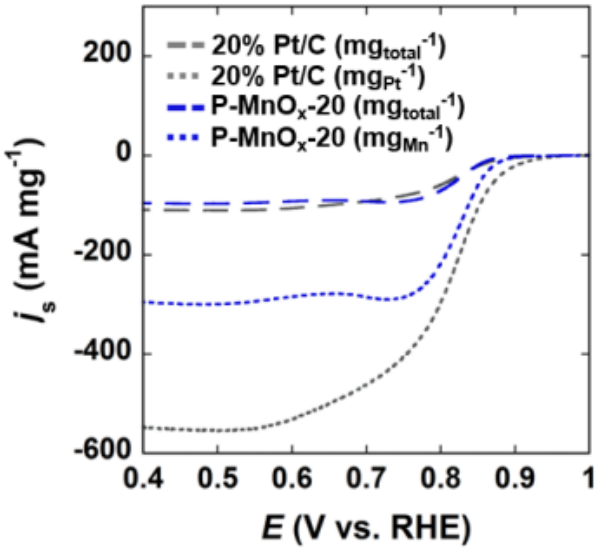

Synergistic activity of PEDOT/MnO_x:

increased *n* value
intrinsic ORR potentials shift by >0.2 V
decreased ORR charge transfer resistance
intimate polymer/active site contact

Bifunctional $Ni_xCo_{3-x}O_4$ for ORR/OER

Sandia National Laboratories

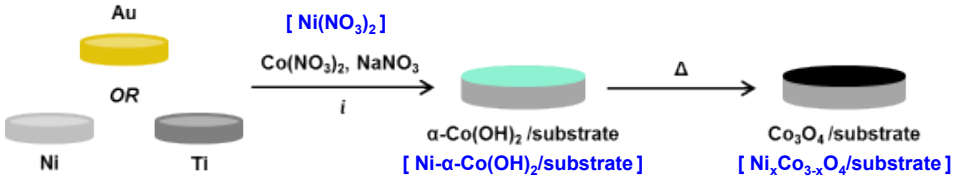

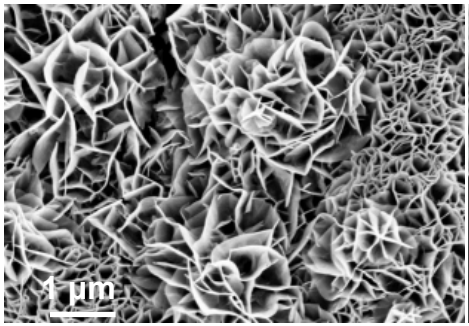

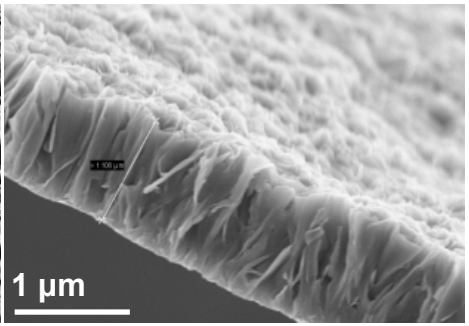

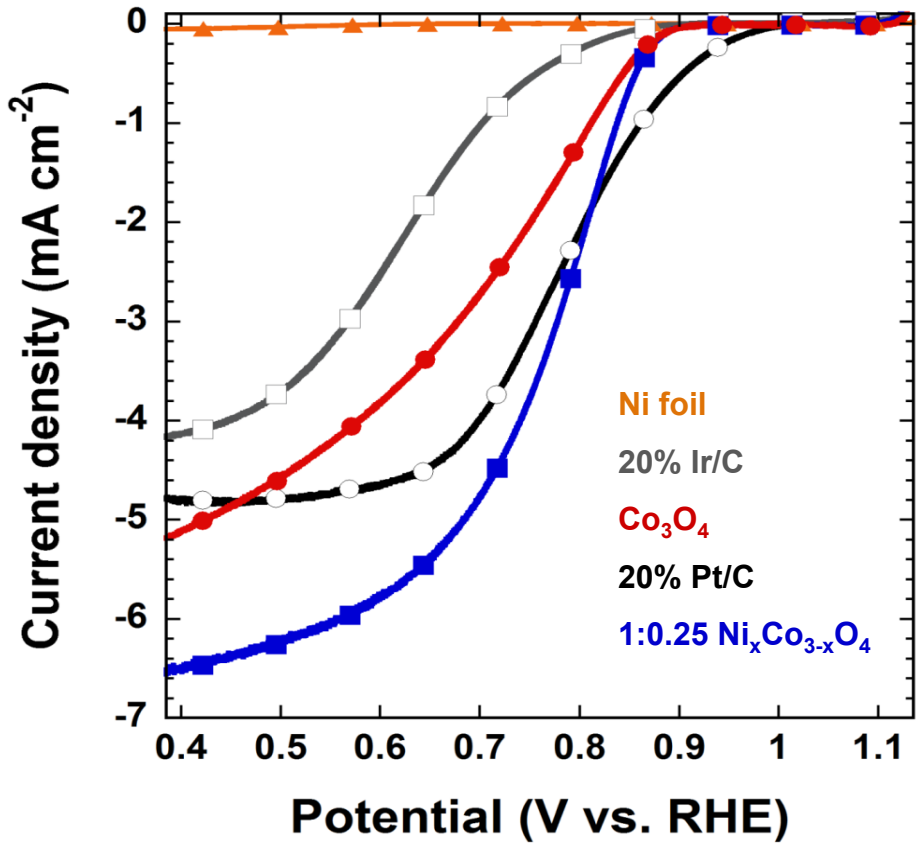

$$ORR:\ O_2 + 2H_2O + 4e^- \longrightarrow 4OH^-$$

Bifunctional $Ni_xCo_{3-x}O_4$	Catalyst loading (mg cm^{-2})	BET Surface Area ($m^2\ g^{-1}$)	ORR: E(V) at I= -3 mA cm^{-2}	ORR Onset (V)
1:0.25 $Ni_xCo_{3-x}O_4$	0.127	99.8	0.79	0.88
$NiCo_2O_4$ Spinel NWAs[1]	ND	124	0.75	0.84
Mesoporous $NiCo_2O_4$ /Graphene [2]	0.407	77	0.55	0.86

T. N. Lambert, J. A. Vigil *et al., Chem. Commun.* **2015**, 51, 9511-9514.

Bifunctional $Ni_xCo_{3-x}O_4$ nanostructured films for the ORR and OER

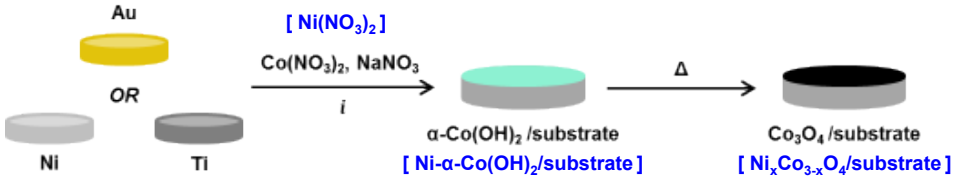

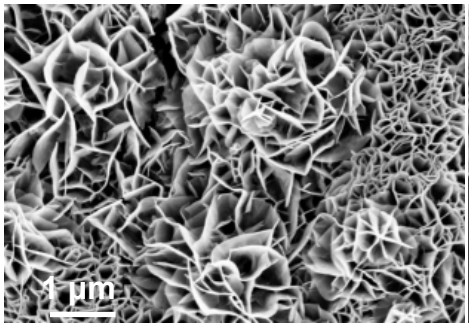

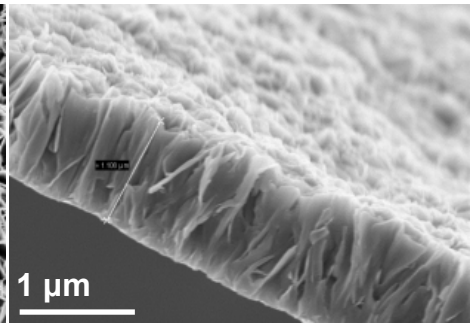

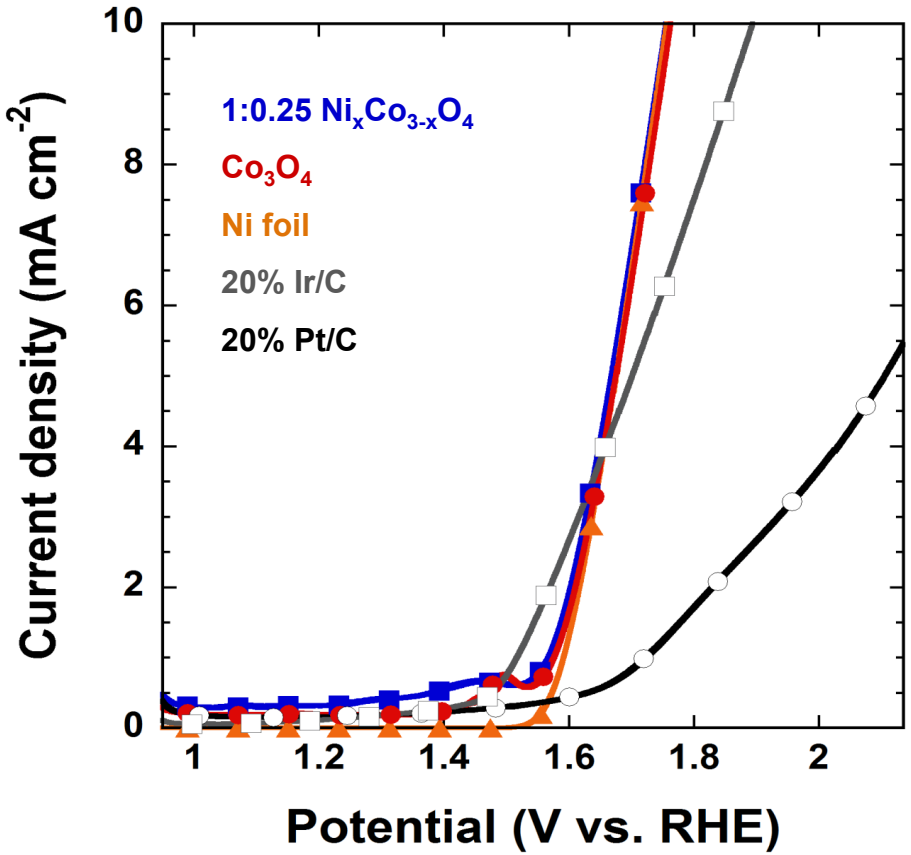

$$OER:\ 4OH^- \longrightarrow O_2 + 2H_2O + 4e^-$$

Bifunctional $Ni_xCo_{3-x}O_4$	Catalyst loading (mg cm^{-2})	BET Surface Area ($m^2\ g^{-1}$)	OER: E(V) at I = 10 mA cm^{-2}	OER Onset (V)
1:0.25 $Ni_xCo_{3-x}O_4$	0.127	99.8	1.75	1.59
$NiCo_2O_4$ Spinel NWAs[1]	ND	124	1.72	1.65
Mesoporous $NiCo_2O_4$ /Graphene [2]	0.407	77	1.69	1.6

T. N. Lambert, J. A. Vigil *et al., Chem. Commun.* **2015**, 51, 9511-9514.

Bifunctional $Ni_xCo_{3-x}O_4$ nanostructured films for the ORR and OER

Sandia National Laboratories

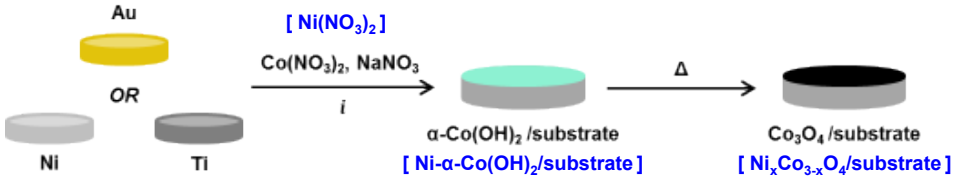

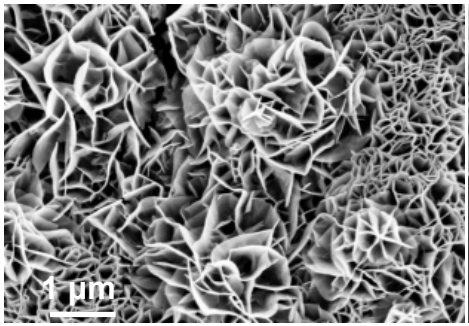

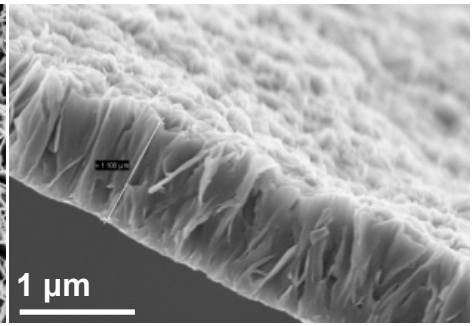

Bifunctional!

$$ORR:\ O_2 + 2H_2O + 4e^- \longrightarrow 4OH^-$$

$$OER:\ 4OH^- \longrightarrow O_2 + 2H_2O + 4e^-$$

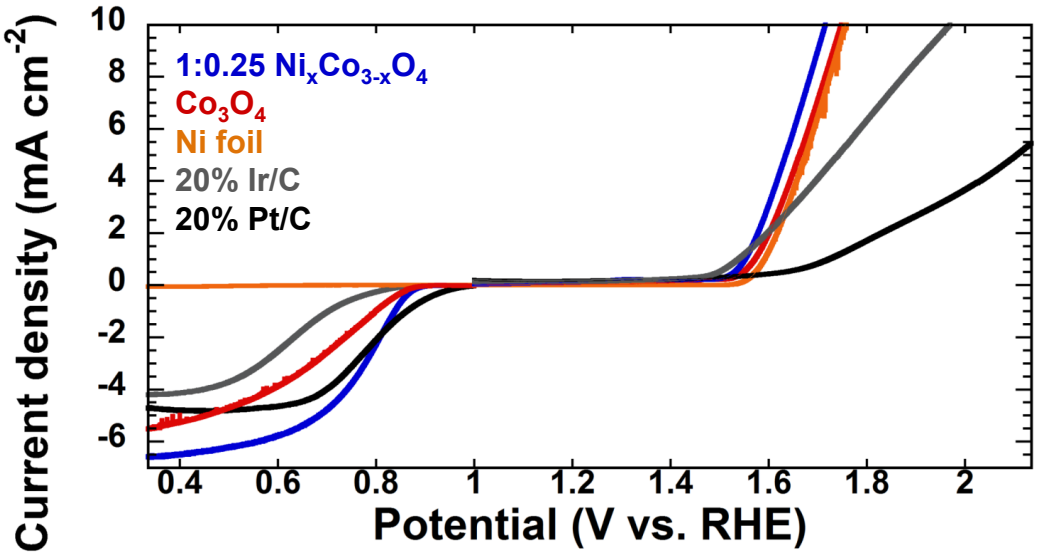

Bifunctional $Ni_xCo_{3-x}O_4$	ORR: E(V) at I= -3 mA cm^{-2}	OER: E(V) at I = 10 mA cm^{-2}	Oxygen Electrode Δ(OER-ORR): E(V)
1:0.25 $Ni_xCo_{3-x}O_4$	0.79	1.75	0.96
$NiCo_2O_4$ Spinel NWAs[1]	0.75	1.72	0.97
Mesoporous $NiCo_2O_4$ /Graphene [2]	0.55	1.69	1.14

T. N. Lambert, J. A. Vigil *et al., Chem. Commun.* **2015**, 51, 9511-9514.

Bifunctional CoP nanostructured films for the HER and OER

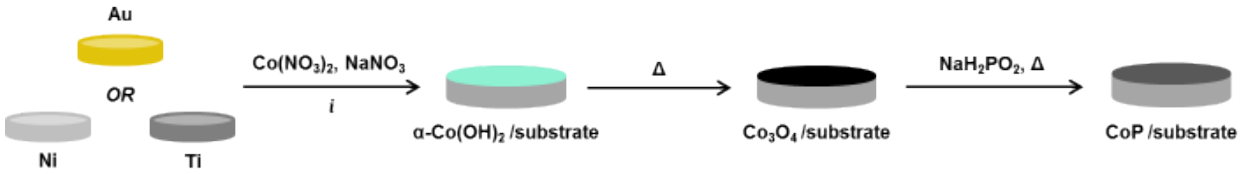

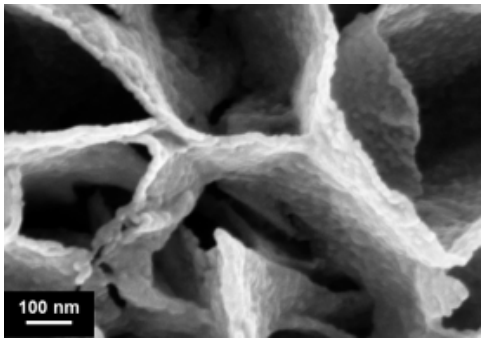

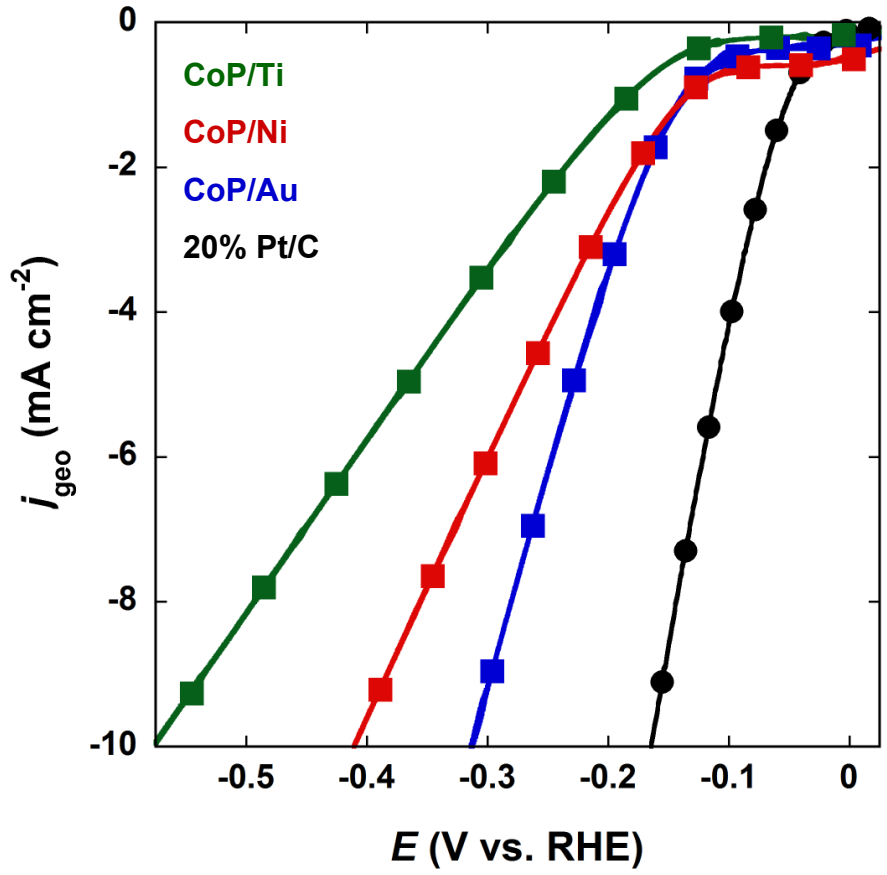

- **Low Tafel slope → efficient HER onset region**
- **Excellent stability: < 5% loss in activity after 100 HER cycles**
- **HER activity in both acidic and basic conditions**

J. A. Vigil and T. N. Lambert, *RSC Adv.*, **5**, 105814 (2015).

Bifunctional CoP nanostructured films for the HER and OER

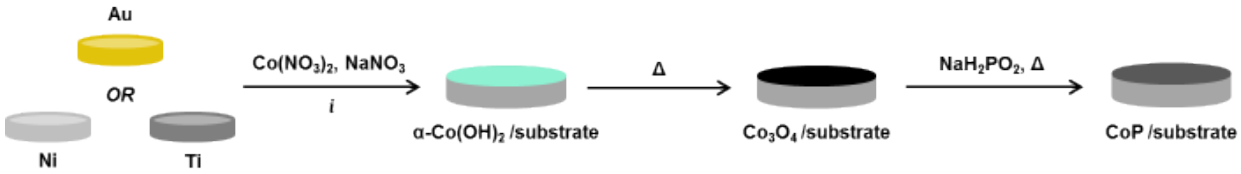

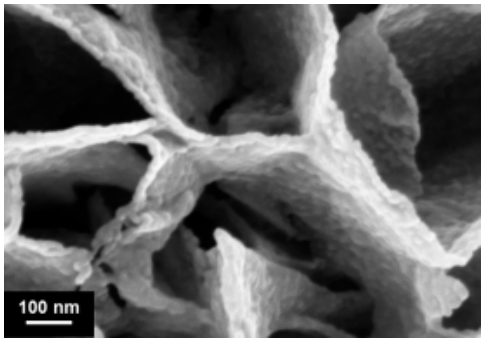

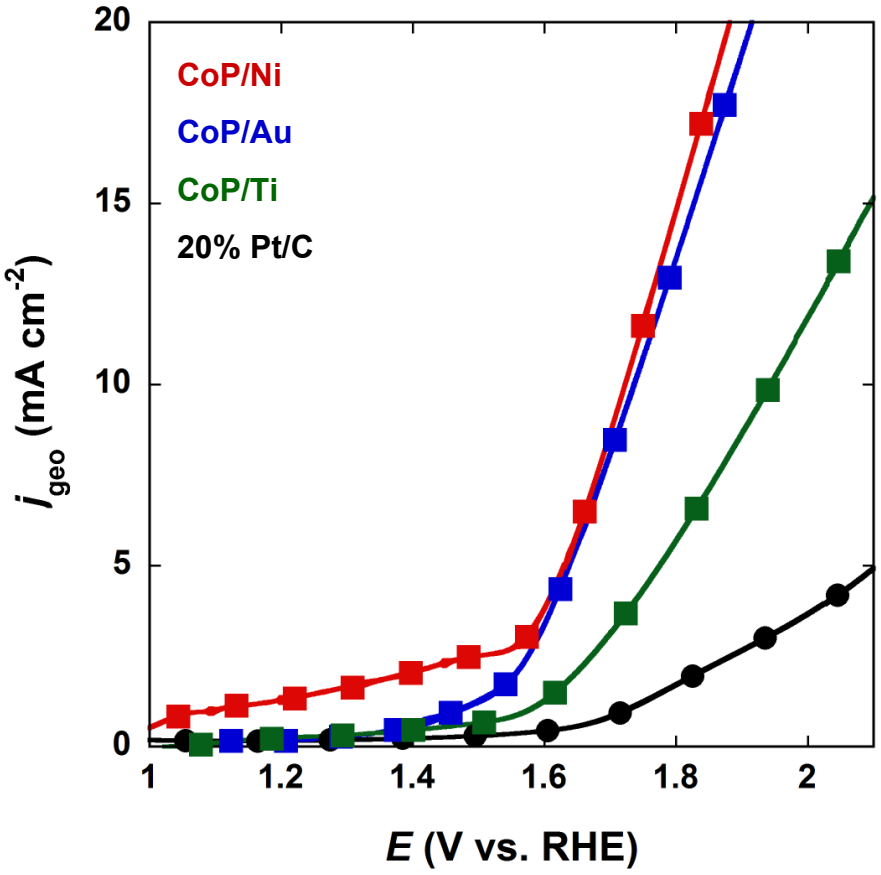

$$OER: 4OH^- \longrightarrow O_2 + 2H_2O + 4e^-$$

- **Early OER onset**
- **Excellent stability: < 5% loss in activity after two hours at OER potential**

J. A. Vigil and T. N. Lambert, *RSC Adv.*, **5**, 105814 (2015).

Bifunctional CoP nanostructured films for the HER and OER

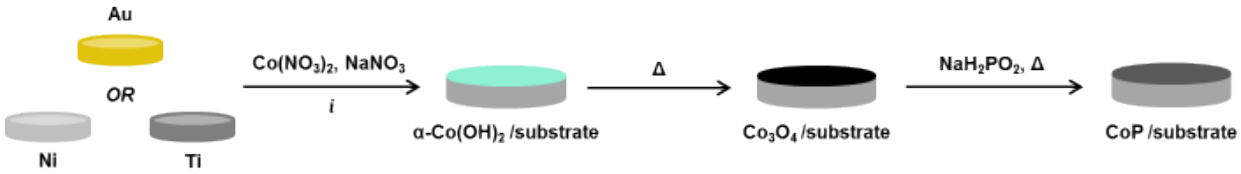

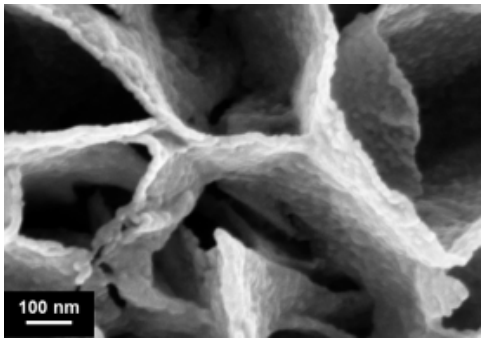

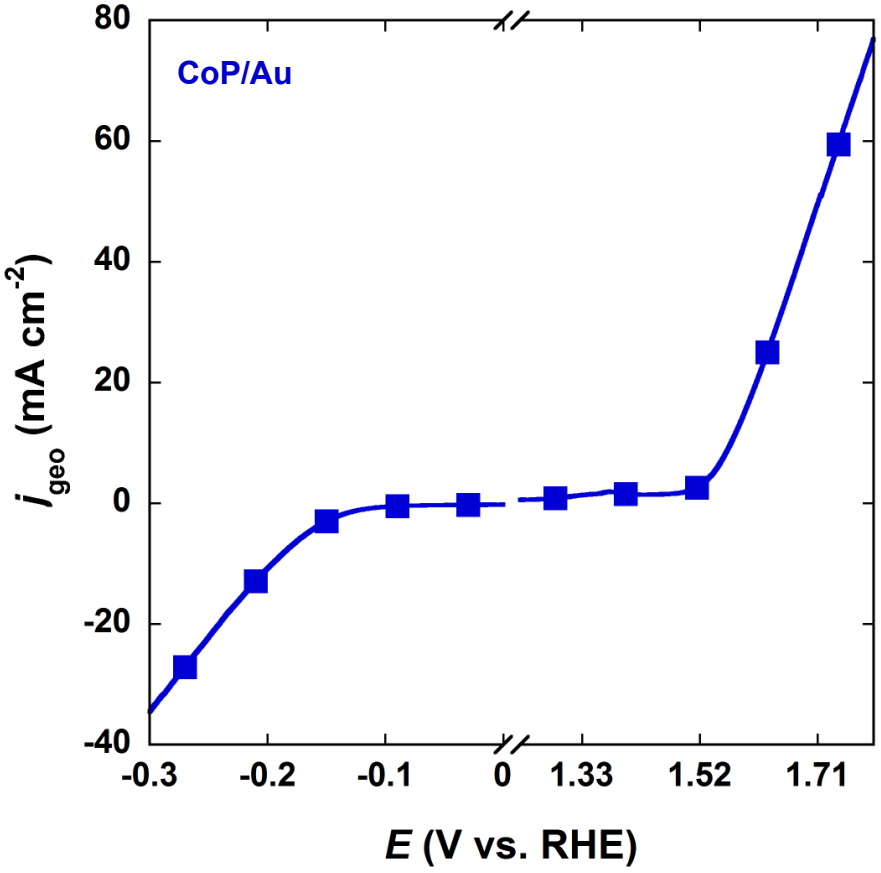

Bifunctional!

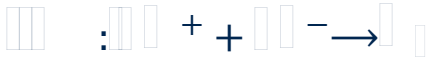

$$OER: 4OH^- \longrightarrow O_2 + 2H_2O + 4e^-$$

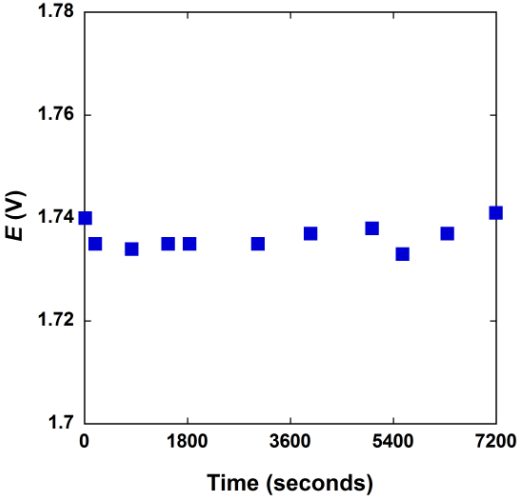

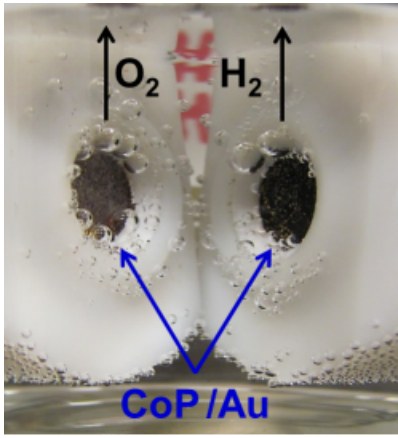

J. A. Vigil and T. N. Lambert, *RSC Adv.*, **5**, 105814 (2015).

Conclusions and future work

Sandia National Laboratories

- Electrodeposition is an extremely versatile method with many applications in energy devices and electrocatalysis.
- Electrodeposited electrocatalysts exhibit key advantages over particle synthesis for both fundamental studies and scalable device integration.

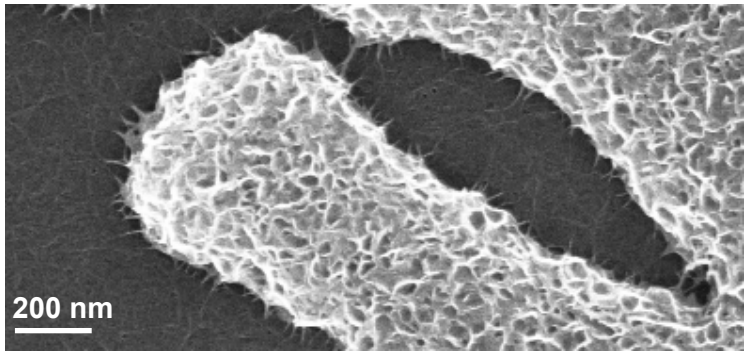

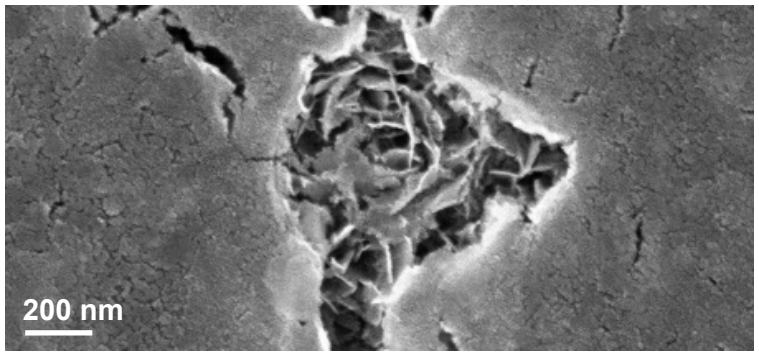

- Electrodeposited, nanostructured films of MnO_x/PEDOT, $Ni_xCo_{3-x}O_4$, and CoP proved to be highly active electrocatalysts for the ORR, ORR/OER, and HER/OER, respectively.
- Future work will be undertaken to further improve these three systems, investigate device integration, and identify new materials to be electrodeposited with potential as active electrocatalysts.

Acknowledgements

- **Sandia National Laboratories Laboratory Directed Research and Development, Department of Energy**

- **Dr. Timothy N. Lambert**

- **Lambert group members (L to R)**
  - Me (UNM/SNL)
  - Ben Christensen, (Cal Poly)
  - Dr. Tim Lambert (SNL)
  - Collin Delker (SNL/CINT)
  - Suzanne White (U. Oklahoma)
  - Maria Kelly (UNM/SNL)

  (Other collaborators)
  - Bonnie McKenzie, Michael Brumbach, Mark Rodriguez (SNL)

Danae Davis, M.S. (SNL)

Kaitlyn Eldred (UT Austin)

- ***The American Chemical Society Division of Inorganic Chemistry***

Sandia National Laboratories

Questions?

Thank you!

Electrocatalysis in energy devices

Sandia National Laboratories

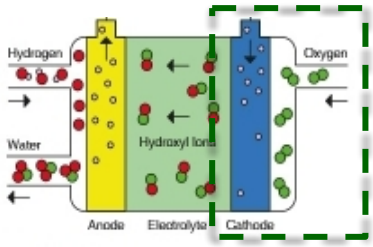

Fuel cell schematic

Alkaline fuel cell:

Anode: $2H_2 + 4OH^- \rightarrow 4H_2O + 4e^-$

Cathode: $O_2 + 2H_2O + 4e^- \rightarrow 4OH^-$ — Oxygen Reduction Reaction (ORR)

Overall: $2H_2 + O_2 \rightarrow 2H_2O$

Secondary metal-air battery (e.g. Zn-air):

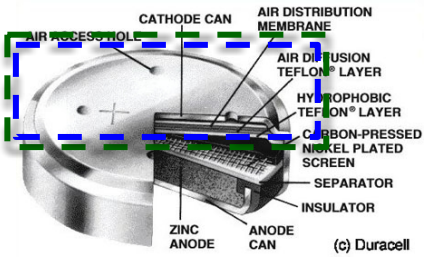

Zn-air battery schematic

Discharge

Anode: $2Zn_{(s)} \rightarrow 2Zn^{2+} + 4e^-$

Cathode: $O_2 + 2H_2O + 4e^- \rightarrow 4OH^-$ — ORR

Overall: $2Zn_{(s)} + O_2 + 2H_2O \rightarrow 2Zn^{2+} + 4OH^-$

Charge

Anode: $2Zn^{2+} + 4e^- \rightarrow 2Zn_{(s)}$

Cathode: $4OH^- \rightarrow O_2 + 2H_2O + 4e^-$ — Oxygen Evolution Reaction (OER)

Overall: $2Zn^{2+} + 4OH^- \rightarrow 2Zn_{(s)} + O_2 + 2H_2O$

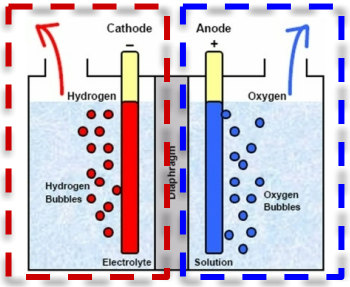

Electrolyzer schematic

Alkaline Electrolyzer:

Anode: $4OH^- \rightarrow O_2 + 2H_2O + 4e^-$ — OER

Cathode: $4H_2O + 4e^- \rightarrow 2H_2 + 4OH^-$ — Hydrogen Evolution Reaction (HER)

Overall: $2H_2O \rightarrow 2H_2 + O_2$

Rational design of electrocatalyst materials

Sandia National Laboratories

ORR

$$O_2 + 2H_2O + 4e^- \underset{OER}{\overset{ORR}{\rightleftharpoons}} 4OH^-$$

- E_0 = 1.23 V vs. RHE
- commercial benchmark catalysts: Pt, Pt/C

OER

$$4OH^- \longrightarrow O_2 + 2H_2O + 4e^-$$

- E_0 = 1.23 V vs. RHE
- commercial benchmark catalysts: Ir, IrO_x, Ru

HER

$$2\square^+ + 2\square^- \longrightarrow \square_2$$

- E_0 = 0 V vs. RHE
- commercial benchmark catalysts: Pt

Abundant, economically viable materials

- **Non-precious metals and non-metals**
- **Easily prepared and scalable**

Oxygen/hydrogen catalytic activity

- **Oxides/hydroxides for ORR/OER**
- **Phosphides/sulfides for HER**
- **Bifunctionality**

Nanoscale and high surface area structures

- **More active catalytic sites**
- **High mass efficiency**

Importance of O_2 Electrochemistry

Sandia National Laboratories

A. Multi-electron ceramic/air batteries (Primary)

1. $VP + 16\ OH^- \Rightarrow VO_4^{3-} + PO_4^{3-} + 8\ H_2O + 10\ e^-$; $E^0 = 1.07$ V vs NHE
2. $O_2 + 2\ H_2O + 4\ e^- \Rightarrow 4\ OH^-$; $E^0 = 0.40$ V vs NHE
3. $VP + 6\ OH^- + 5/2\ O_2 \Rightarrow VO_4^{3-} + PO_4^{3-} + 3\ H_2O$; $E^o = 1.47$ V

VP/air ~ 4.3 kWh L^{-1}
vs.
Gasoline 2.7 kWh L^{-1}

TN Lambert *et al. Chem. Commun.* **2011** *47*, 9597-9599.

B. Sodium/air batteries (Secondary)

Anodic half-reaction: $Na = Na^+ + e^-$ $E^0 = 0.00$ V/Na
Cathodic half-reaction: $O_2 + 2H_2O + 4e^- = 4\ OH^-$ $E^0 = +3.1$ V/Na
Full cell reaction: $4Na + O_2 + 2H_2O = 4Na + 4OH^-$

Na/air ~ 1690 Wh kg^{-1}
vs.
Li-ion 200-250 Wh kg^{-1}

Review: J. Power Sources **2011**, *196(16)*, pp 6835-6840

C. Alkaline Fuel Cells (Bi-directional beneficial)

Anodic half-reaction: $2\ H_2 + 4\ OH^- \Rightarrow 4H_2O + 4e^-$
Cathodic half-reaction: $O_2 + 2\ H_2O + 4e^- \Rightarrow 4\ OH^-$
Full cell reaction: $2\ H_2 + O_2 \Rightarrow 2\ H_2O$

Proc. Nat. Acad. Sci. **2008**, *105(52)*, pp 20611-20614

D. Solar Fuels Synthesis

Fuel Generation: $2H^+ + 2e^- \Rightarrow H_2$ $E^0 = 0.00$ V/RHE
or $CO_2 + 6H^+ + 6e^- \Rightarrow CH_3OH + H_2O$ $E^0 = +0.05$ V/RHE

Source of protons: $2H_2O \Rightarrow 2O_2 + 4H^+ + 4e^-$ $E^0 = +1.23$ V/RHE **Water Electrolysis**

Gorlin *et al. J. Am. Chem. Soc.* **2010**, 132, 13612-13614

Most effective catalysts are based on precious metals = rare, expensive

MnO_x/PEDOT composite thin films for the ORR

Sandia National Laboratories

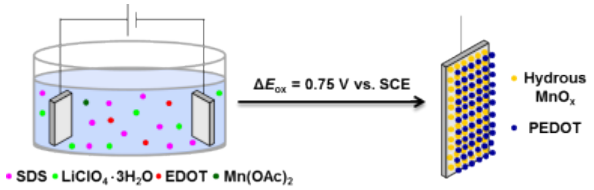

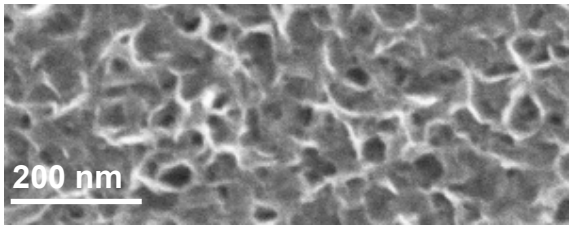

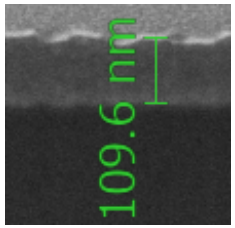

$$ORR: O_2 + 2H_2O + 4e^- \longrightarrow 4OH^-$$

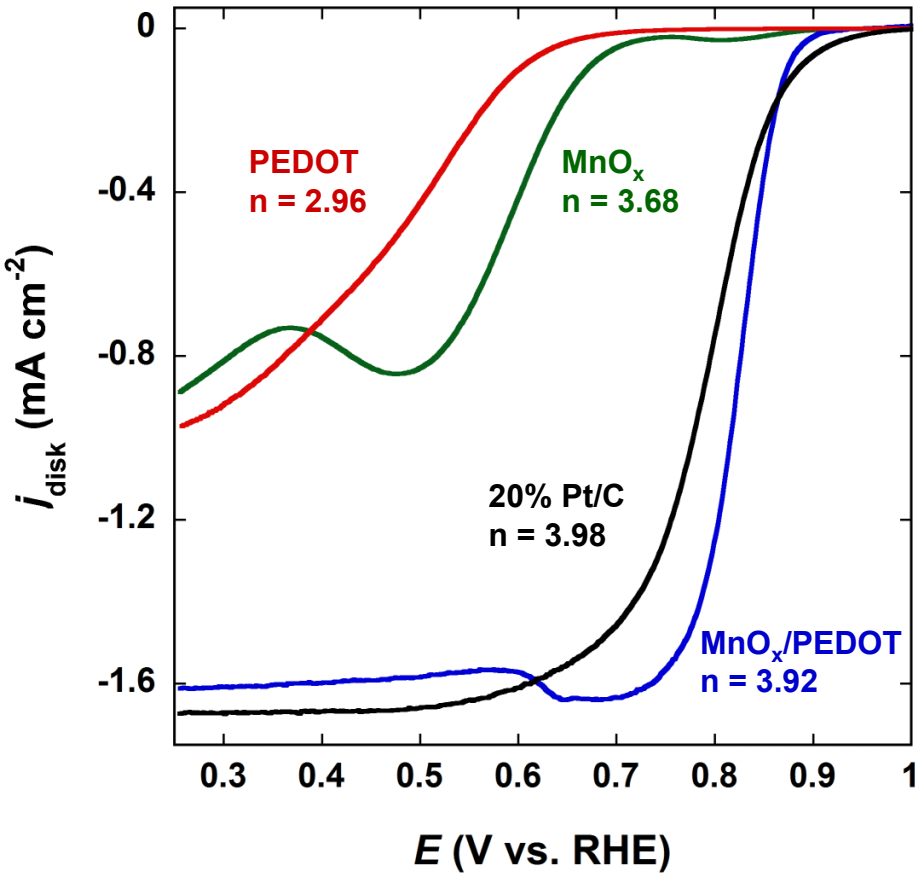

- **MnO_x/PEDOT improvement over MnO_x and PEDOT alone → synergism/coupling effect**
- **Electrochemical impedance used to quantify charge transfer characteristics:**

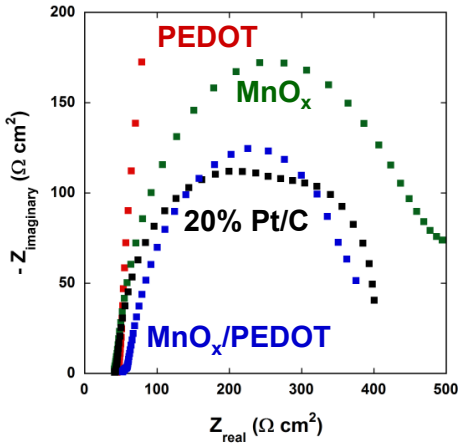

Rationalizing the MnO_x/PEDOT synergism

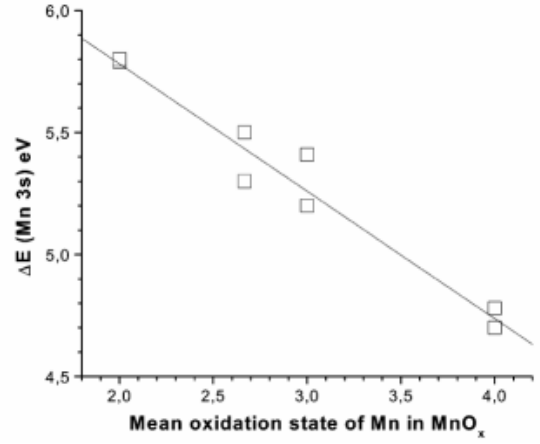

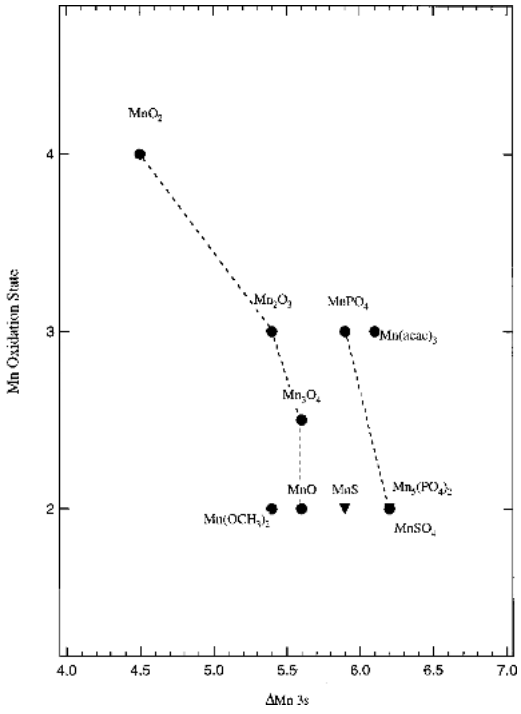

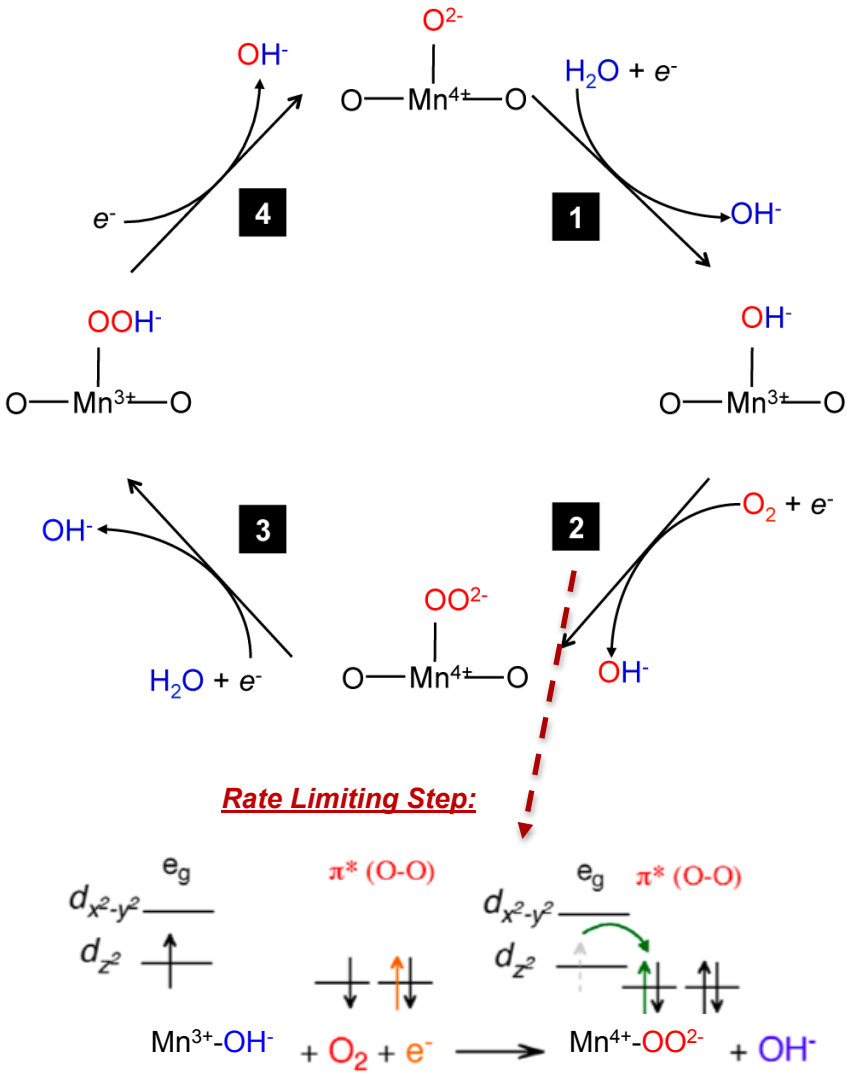

Chem. Mater. **2002,** *14,* 3946-3952 *J. Vac. Sci. Technol. A* **18**, 1072 (2000) D. J. Davis *et al. J. Phys. Chem. C.* **2014**, *118*, 17342-17350.

Rationalizing the MnO_x/PEDOT synergism

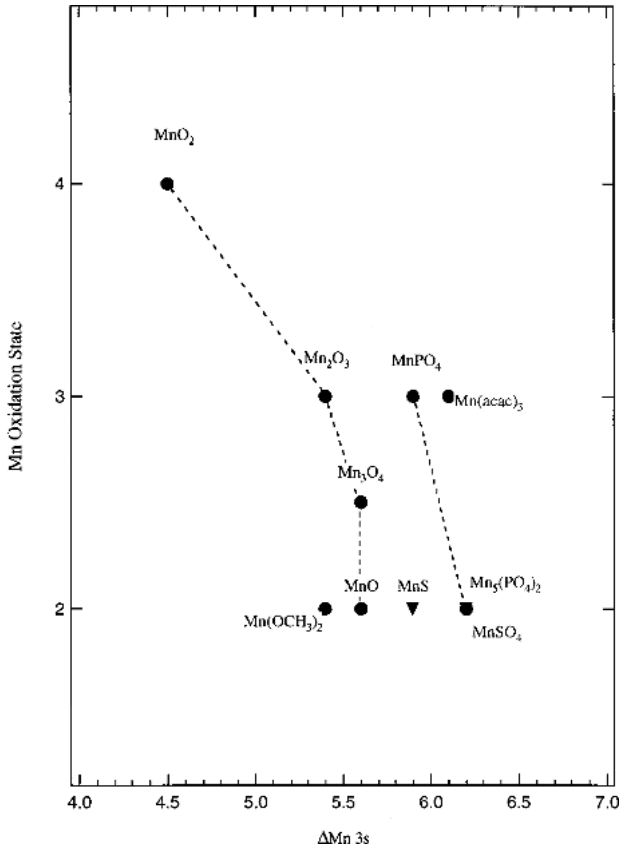

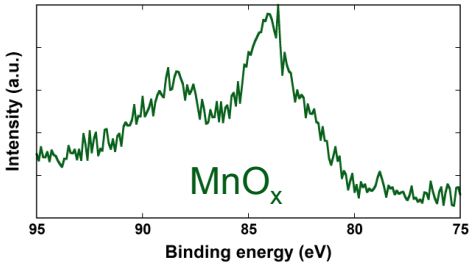

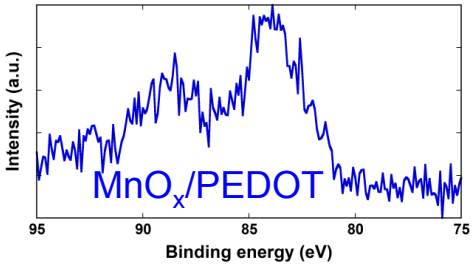

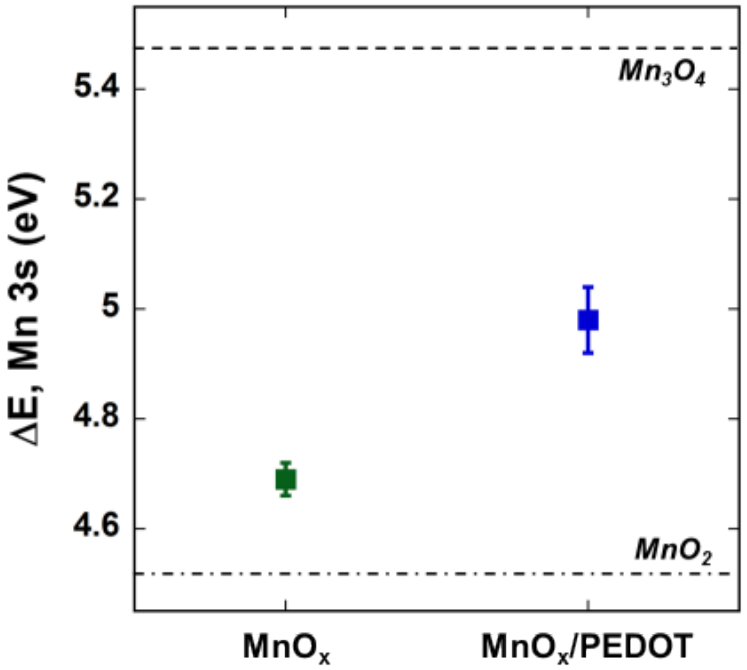

Comparing to other known PEDOT electrocatalysts

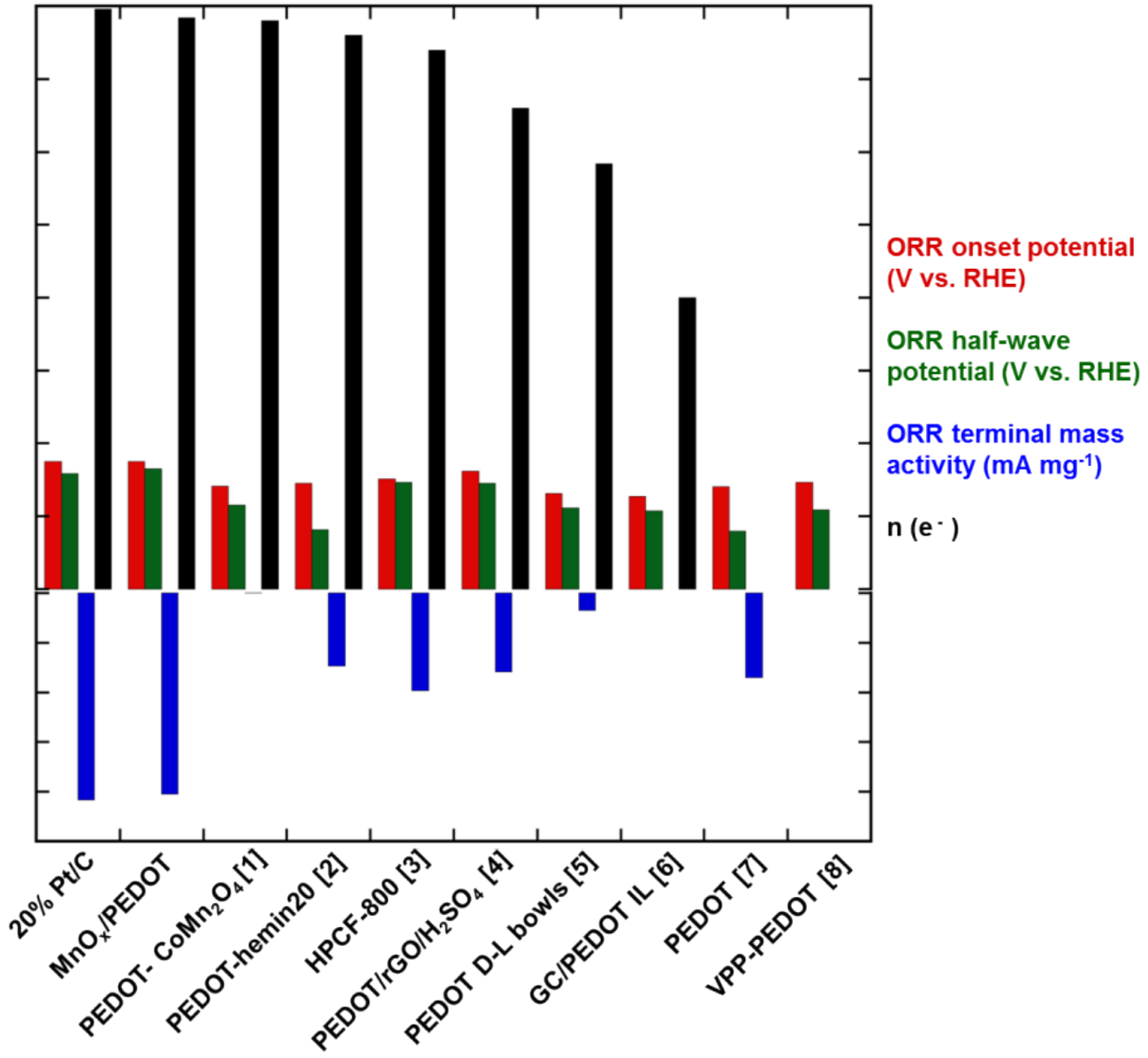

- Highest reported activity from a PEDOT-based ORR catalyst
- Competitive with commercial 20% Pt/C

J. A. Vigil *et al. ACS Appl. Mater. Interfaces* **2015**, 7 (41), 22745–22750.

Why Cobalt? Bifunctionality

Sandia National Laboratories

Oxygen reduction/evolution (ORR/OER)

$$O_2 + 2H_2O + 4e^- \underset{\text{OER}}{\overset{\text{ORR}}{\rightleftharpoons}} 4OH^- \qquad E^o = +1.23 \text{ V vs. RHE}$$

Commercial catalyst materials: ***Pt, Pt/C, Ir, IrO_x, Ru ($$)***

Water electrolysis (HER/OER)

$$2H_2O \underset{\text{OER}}{\overset{\text{ORR}}{\rightleftharpoons}} O_2 + 2H_2 \qquad E^o = 0 \text{ V vs. RHE}$$

Commercial catalyst materials: ***Pt, Ir, IrO_x, Ru ($$), Ni***

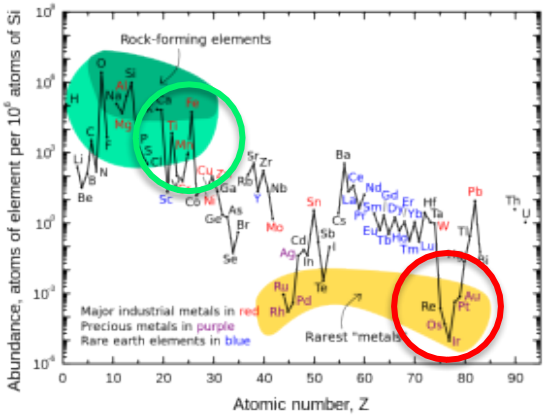

Co abundance